Finite Element Analysis of Square Spiral Inductors Based on MEMS Technology

Yaowu Xu[1], Daisheng Xu[1,*]

[1]School of Optoelectronics & Communication Engineering, Xiamen University of Technology, Xiamen, 361024, China
[*]Corresponding author: xudaisheng@xmut.edu.cn

Abstract: Inductors play a crucial role in signal processing, current stabilization, and suppression of electromagnetic interference, making them essential components in integrated filtering circuits. However, traditional inductors suffer from limitations such as low frequency bandwidth, large size, and low power. Additionally, they are constrained by manufacturing barriers associated with magnetic materials. This paper utilizes the finite element simulation method to establish a model of an integrated square spiral inductor based on Micro-Electrode-Mechanical System (MEMS) technology. Through three-dimensional finite element simulation analysis, the spatial magnetic field and potential distribution of the square spiral inductor are intuitively demonstrated, and the resistance and inductance values of the simulation model are obtained.

1. Introduction

With the rapid development of the electronics industry, competition in various fields has become increasingly intense. Integrated circuits, as the core of the electronics industry, play a crucial role in computer technology, automotive, medical, aerospace, and military fields. Inductors are an indispensable part of integrated circuits, aiming to eliminate unnecessary signals such as noise and interference, thereby improving the quality and reliability of signals.

Currently, the development of inductors faces several challenges. These include selecting suitable magnetic materials and manufacturing processes, reducing manufacturing costs, improving size and integration, and addressing the difficulties in designing high-frequency characteristics. These factors to some extent restrict the progress of inductor technology.

The study of inductors has always been one of the hot and challenging areas in the field of the electronics industry. With the continuous advancement of integrated circuit technology, the demand for inductors has been increasing. To address these challenges, researchers have proposed various methods, such as RF inductors [1], power inductors [2], magnetic inductors [3], non-magnetic inductors [4], through-hole inductors [5], and chip inductors [6]. These approaches have achieved remarkable results in inductor design. However, the aforementioned types of inductors still have some issues that need to be addressed. For example, RF inductors are highly sensitive to operating frequencies and require precise design and matching. They are also susceptible to electromagnetic interference, which can affect their performance and stability. Power inductors typically require larger

coils and materials to handle high-power currents, resulting in a larger size, heavier weight, and higher production costs. The magnetic field generated by power inductors may also interfere with surrounding electronic devices and circuits. Magnetic inductors rely on magnetic materials and coils, which often have a larger size and heavier weight. Additionally, certain magnetic materials are sensitive to temperature changes, which can cause variations in inductance with temperature fluctuations. Non-magnetic inductors, which use non-magnetic materials, have lower inductance values and poorer electromagnetic shielding performance. They are only suitable for specific applications. Through-hole inductors require insertion into circuit boards or device slots, occupying a larger space. The connection method of through-hole inductors can also be sensitive to vibrations and shocks. When devices are subjected to external forces, it can lead to the loosening or disconnection of the inductor. Due to limitations in size and structure, through-hole inductors may have restrictions on their inductance values and power capacity, which may prevent them from meeting the requirements of certain high-demand applications. In the case of chip inductors, their manufacturing process and material costs are higher compared to traditional wire coil inductors, resulting in relatively higher prices. The presence of multiple layers and insulation layers in inductors can result in some losses, potentially leading to power dissipation. Additionally, chip inductors have a small size and relatively poor heat dissipation conditions, which limits their selection range, making them suitable primarily for low-power and medium-power applications. They are not well-suited for high-power applications.

In recent years, researchers have proposed numerous innovative advancements in improving the existing model structure. For instance, Xiangu et al. [7] developed a method that involved winding copper wire on a small ceramic core and soldering the copper wire to the ceramic core electrode. The product's backside was then coated with adhesive. The approach offers advantages such as small size and high self-resonant frequency. However, this method may encounter challenges related to complex processes, poor repairability, uneven adhesive coating, and weak mechanical strength. In their work, Chen Yang et al. [8] introduced a method that combines system-level packaging integration with glass as the medium. They demonstrated that DC voltage converters based on glass inductors exhibit higher power conversion efficiency. The approach enhances system integration, operational speed, and reduces power consumption. It also offers advantages such as fewer process steps and high stability. However, this method still faces challenges related to mechanical fragility and size limitations. Zheng Lu et al. [9] utilized the spin-coating method to prepare NiZn ferrite thin films and developed annular thin film inductors based on semiconductor processes and spin-coating. Their research revealed that the thickness of the magnetic film, coil thickness, and coil width have an impact on the performance of the thin film inductor. By optimizing these parameters, the inductor's performance can be improved. However, this method may face challenges such as frequency magnetic energy limitations, complex preparation processes, and inconsistent film quality. Gao Qi et al. [10] combined magnetic powders with epoxy resin to produce composite magnetic materials, and integrated them with advanced printed circuit board fabrication processes to create integrated spiral coil magnetic core inductors with high inductance density and quality factor. Through a series of characterizations, this method has demonstrated reliability and innovation, making it highly suitable for board-level packaging in power management modules.

Based on the analysis above, it is evident that the design of an inductor is not fixed but rather needs to be adjusted according to specific requirements. In practical applications, we need to choose the appropriate type of inductor based on the specific circumstances. Different types of inductors have their own characteristics and advantages. Therefore, when selecting an inductor, it is essential to consider application requirements, performance specifications, and design complexity, among other factors. Flexibly choosing the appropriate type of inductor can ensure that the system meets the expected functionality and enhances its performance and efficiency. In this study, a model of an

integrated square spiral inductor based on MEMS processes was constructed using finite element analysis. The process involved generating a geometric model of a square spiral hollow inductor using simulation software, specifying material parameters, and establishing a material model. The electromagnetic field model under a constant current was built using the electromagnetic field interface provided by the software. The magnetic flux density and potential distribution were obtained by calculating the simulation model. The resistance value and inductance were derived from the calculation results. Through finite element analysis and simulation methods, the integrated square spiral inductor model based on MEMS processes was validated, demonstrating good inductance performance and dimensional stability. This enables the design of filters that meet specific requirements more effectively.

2. Theoretical Summary

2.1 Principles of Filter Integrated Circuit Packaging Design

Integrated circuits are electronic components that are integrated together using semiconductor processes to form circuits with specific functions. The production process mainly consists of three stages: design, fabrication, and testing. As shown in Fig. 1, the design stage of integrated circuits can be divided into two parts: front-end design and back-end design. Integrated circuit design is the process of transforming the design requirements of system, logic, and performance into specific physical layouts. It primarily involves stages such as logic design, circuit design, and layout design. The final circuit design is then fabricated into masks and proceeds to the next manufacturing stage. The manufacturing process is further divided into two parts: wafer fabrication and wafer processing. Wafer fabrication involves transforming the design layout into masks and then etching the circuit pattern onto the silicon wafer, thereby forming the circuit on the bare wafer, completing the construction of the entire circuit chip. Wafer processing is the process of building a complete integrated circuit chip on the prepared wafer material. It primarily includes a series of process steps such as mask fabrication, wafer preparation, deposition, photolithography, etching, ion implantation, metallization, and packaging. The final testing stage consists of packaging and testing. Packaging involves cutting the wafer, wire bonding, and encapsulating the chip to establish electrical connections with external devices. During this process, the integrated circuit chip is placed inside a protective casing to prevent physical damage or chemical corrosion. The qualified products that pass testing are used as final products and deployed in downstream applications.
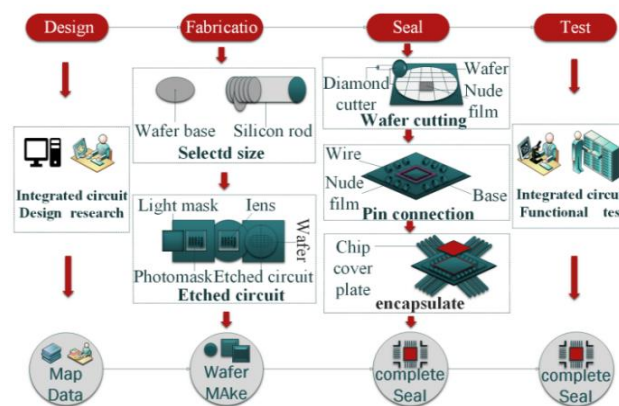
Figure 1: Integrated Circuit Fabrication Process

Inductors play a crucial role in filter integrated circuits. Modern electronic devices often require signal processing and filtering to eliminate noise and unwanted frequency components while retaining

the desired signals. These processing and filtering functions are typically achieved using filters. As shown in Fig. 2, low-pass, high-pass, band-pass, and band-stop filters are the four most commonly used types of filters in integrated circuits. A low-pass filter allows signals below a specific cutoff frequency to pass through the filter while attenuating higher-frequency signals. Conversely, a high-pass filter attenuates low-frequency signals and allows signals above a specific cutoff frequency to pass through. A band-pass filter permits signals within a specific frequency range to pass through the filter while attenuating signals outside that range. Finally, a band-stop filter selectively attenuates signals within a specific frequency range while allowing other frequencies to pass through the filter.
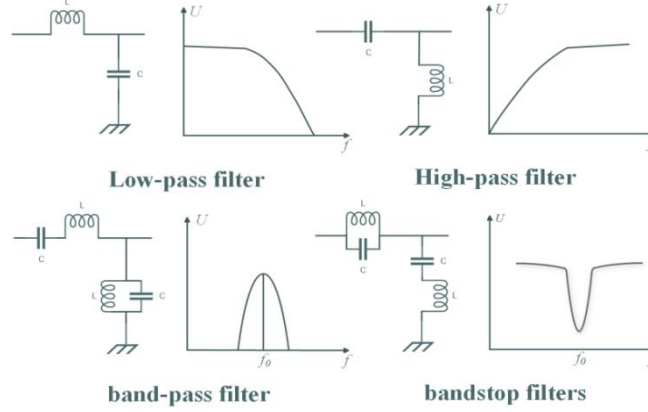
Figure 2: Circuit Topology

2.2 Principles of Simulation for Square Spiral Inductor

The simulation model for the inductor is based on MEMS manufacturing processes. MEMS manufacturing processes refer to the fabrication techniques for microstructures ranging from millimeters to nanometers in scale. It originated from semiconductor and microelectronics processes and is an independent intelligent system capable of large-scale production. The dimensions of MEMS systems are typically in the range of a few millimeters or even smaller, while their internal structures are typically at the micron or even nanometer level. Due to the numerous advantages of MEMS, it finds wide applications in various industrial fields. Firstly, due to the precision and controllability of MEMS manufacturing processes, it enables the design of small-sized and highly integrated devices. This gives MEMS systems significant advantages in terms of volume and weight, allowing for the realization of complex functionalities within limited space. Secondly, MEMS devices typically exhibit low power consumption and fast response characteristics, making them widely utilized in areas such as mobile devices, sensors, and wireless communications. Furthermore, MEMS technology provides solutions for manufacturing high-performance inertial navigation systems, optical devices, biomedical sensors, and more.

The square spiral inductor model utilizes the electromagnetic field physics interface, wherein Ampere's law and current conservation are the main features. The model takes into account the current conservation equation, boundary conditions, and external currents for modeling electric and magnetic fields. The control equations of the electromagnetic field model are as follows:

$$\nabla \cdot \boldsymbol{J} = 0 \tag{1}$$

$$\nabla \times \boldsymbol{H} = \boldsymbol{J} \tag{2}$$

$$\boldsymbol{B} = \nabla \times \boldsymbol{A} \tag{3}$$

$$\boldsymbol{E} = -\nabla \boldsymbol{A} \tag{4}$$

$$J = \sigma E + \sigma V \times B + J_e \tag{5}$$

Where: J represents the current density. H represents the magnetic field intensity, σ represents the electrical conductivity of the material, E represents the electric field intensity, J_e represents the induced current density, V represents the electric potential, B represents the magnetic flux density, A represents the magnetic vector potential

3. Model Construction

3.1 Model Definition

(1) Structural Model Establishment.In this study, a square spiral inductor is designed using finite element analysis software. The aim is to calculate the inductance value of the spiral inductor. Based on the obtained magnetic field values from the simulation model, the inductance coefficient L can be calculated using the following relationship.

$$L = \frac{2W_m}{I^2} \tag{6}$$

Where W_m represents magnetic energy and I represents current. By applying terminal boundary conditions and setting the current to 1 Ampere, the inductance value L can be calculated using the formula. The model equation is as follows:

$$-\nabla \cdot (\sigma \nabla V - J_e) = 0 \tag{7}$$

$$\nabla \times (\mu_0^{-1} \mu_r^{-1} \nabla \times A) + \sigma \nabla V = J_e \tag{8}$$

In the above equation, σ represents the electrical conductivity, A is the magnetic vector potential, V is the scalar electric potential, J_e is the externally generated current density vector, μ_0 is the magnetic permeability of vacuum, and μ_r is the relative magnetic permeability. The constitutive relationship is specified by the following expressions:

$$B = \mu_0 \mu_r H \tag{9}$$

Where H represents the magnetic field. The structure of the inductor is shown in Fig. 3, and the geometric parameters are indicated in the figure. D_i represents the inner diameter of the inductor, D_0 represents the outer diameter of the inductor, W represents the line width, and S represents the line spacing.
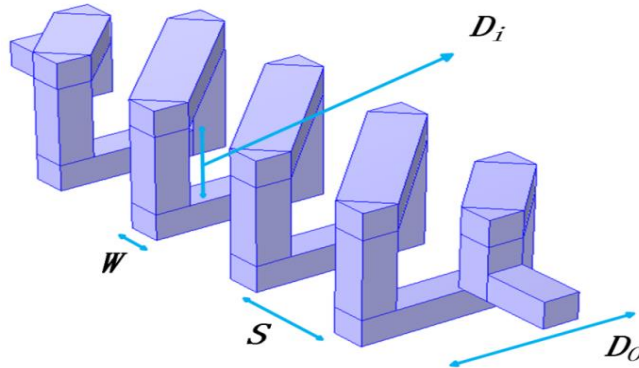
Figure 3: Spiral Inductor Model

(2) Parameter Configuration and Material Properties. The material properties used in different parts of the spiral inductor model are provided in Table 1. The magnetic core material is pure copper,

while the air region is modeled using a simplified air material model. To improve the stability of the iterative solution process, a non-zero low electrical conductivity is assigned to the surrounding air domain of the spiral inductor. This allows for neglecting the effect of zero electrical conductivity in the air domain on the model solution if the geometric dimensions of the conductor are much smaller than the skin depth of the current flowing through it.

Table 1: Material Properties

Material	Properties		Copper
Air			
Electrical	Conductivity		6e7
1			
Relative	Permittivity		1
1			
Relative	Magnetic	Permeability	1
1			

(3) Meshing and Boundary Condition Settings.In the finite element analysis of the spiral inductor model, a coarse meshing strategy is employed for the air domain, while the port and conductor regions are finely meshed. Coarsening the mesh in the air domain is done to approximate real-world conditions, optimize the model, improve accuracy, accelerate the solving process, and enhance stability. On the other hand, the conductor region is refined to accurately simulate the electromagnetic properties of the conductor and ensure proper boundary conditions and material characteristics. The port region is highly refined to accurately simulate the entry and exit of the electromagnetic field, accurately capture boundary conditions, capture waveguide effects, and minimize numerical errors. This combination of coarse and fine meshing strategies allows for an accurate representation of the electromagnetic behavior of the spiral inductor while optimizing computational resources and maintaining numerical stability.

In general, the outer boundaries of the model are typically set to magnetic insulation and electrical insulation boundary conditions. The governing equations for the magnetic field boundary conditions are as follows:

$$\boldsymbol{n} \times \boldsymbol{A} = 0 \qquad (10)$$

For the conductor boundaries, one end is set to a terminal boundary condition with current type, while the other end is set to a grounded boundary condition. The corresponding equation is:

$$\boldsymbol{V} = 0 \qquad (11)$$

A current of 1 Ampere is applied at the terminal boundary to enter the coil, and the initial values of the current components are set to 0wb/m, and the voltage is set to 0 Volts. By using the given formulas, the inductance value, magnetic flux density, and electric potential distribution can be calculated.The meshing of the inductor is shown in Fig. 4
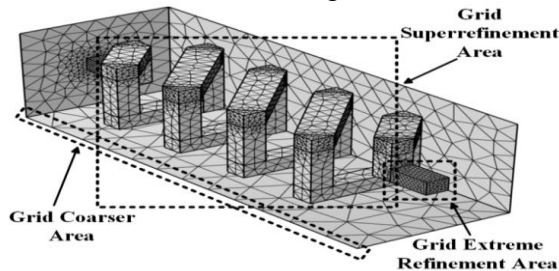
Figure 4: Meshing Diagram of the Spiral Inductor

3.2 Simulation Results Analysis

In the inductor model, a current of 1 Ampere is applied as an external excitation. By utilizing the global computation module, the simulation model of the square spiral inductor yields a resistance value of 1.0743e-3 (Ω) and an inductance value of 2.1182e-14 (H). Fig. 5 displays the magnetic flux density of the inductor. In the magnetic flux density plot, the magnetic flux lines originate from the terminal and flow towards the grounded end. The magnetic flux is uniformly distributed around the entire conductor.
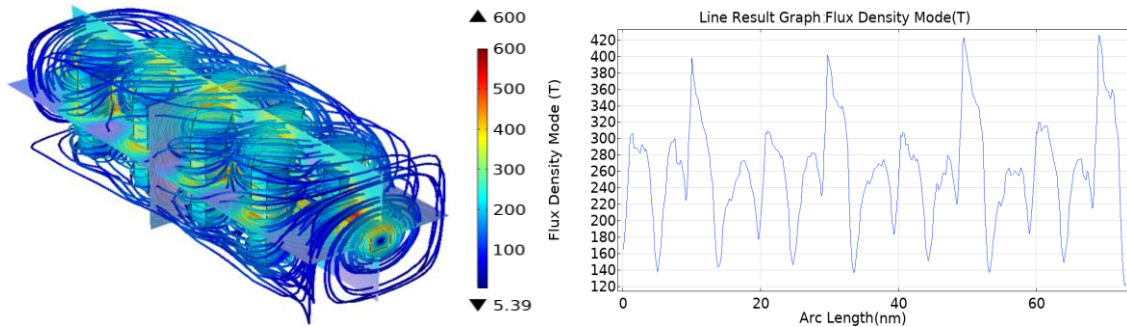
Figure 5: Magnetic Flux Density Plot of the Spiral Inductor

Fig. 6 shows electric potential distribution plot of the inductor. In the electric potential distribution plot of the inductor, the color of the conductor represents its electric potential magnitude, where different colors correspond to different electric potential values. At the end close to the current source, the conductor has a higher electric potential. Additionally, the position near the center of the inductor experiences the maximum magnetic flux passing through it, which aligns with the expected results. The designed square spiral inductor exhibits characteristics of blocking alternating current while allowing direct current to pass through. It also has lower self-resistance when direct current is flowing, demonstrating the typical behavior of an inductor.
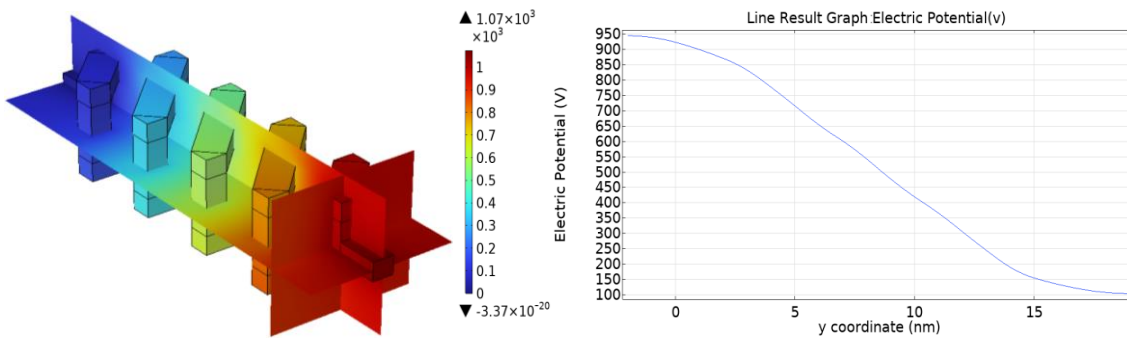
Figure 6: Electric Potential Distribution Plot of the Inductor

Fig. 7 illustrates the distribution of magnetic flux density of the spiral inductor on cross-sections at axial heights of 0, 21, and 0 nanometers. From Fig. 7, it can be observed that at the same axial height within the spiral inductor, the magnetic flux density is approximately equal at various points along the horizontal radial direction. However, due to the presence of end-face effects, the magnetic flux density reaches its maximum value at the end-face. This observation aligns with the conclusions obtained through alternative methods as documented in reference [11].
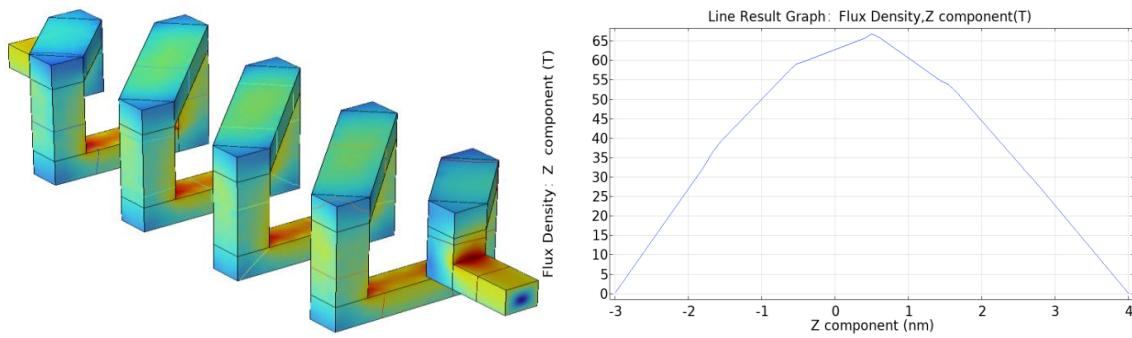
Figure 7: Distribution of Magnetic Flux Density along the Z-axis of the Spiral Inductor.

Fig. 8 illustrates the distribution of magnetic flux density along the Y-axis direction of the spiral inductor. Based on the data in the figure, the magnetic flux density along the axial direction of the spiral inductor is approximately equal and is around 11e-5 Tesla. Due to the influence of the pitch of the spiral inductor, there is a certain amount of magnetic leakage, resulting in a lower magnetic field intensity compared to a tightly wound spiral inductor with the same parameters. The amplitude of the magnetic flux density distribution decreases rapidly towards the axial edges, reaching approximately half of the value at the center. This observation is consistent with the conclusions obtained through experimental testing as documented in reference [12].
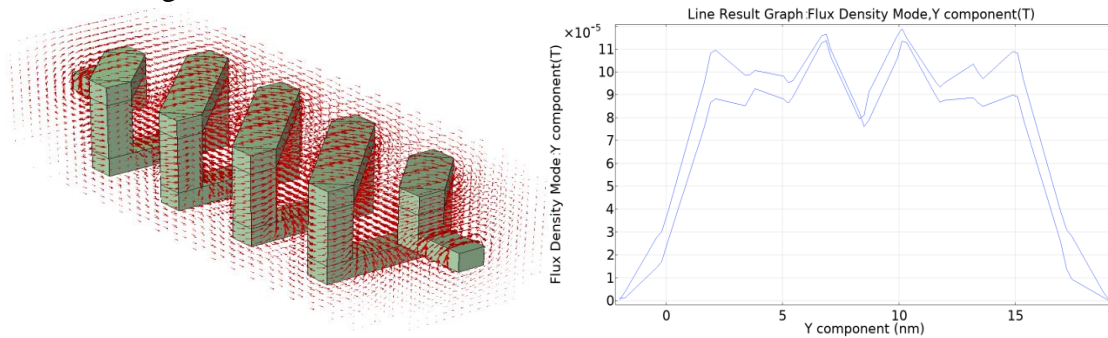
Figure 8: Distribution of Magnetic Flux Density along the Y-axis of the Spiral Inductor

4. Conclusion

This study investigates inductance filter circuits in integrated filter circuits and proposes an integrated square spiral inductor. The validity of the proposed model is verified using finite element simulation methods. The results reveal that the potential increases as it approaches the current input terminal, while the maximum magnetic flux density occurs at the center of the inductor. The distribution of magnetic flux density along the axial edge decreases rapidly, reaching approximately half of the value at the center. Furthermore, the magnetic flux density values along the same axial line height within the square spiral inductor exhibit approximate uniformity in the horizontal radial direction. The proposed model exhibits typical characteristics of an inductor and can be applied to the construction of inductance filter integrated circuits. The simulation results are consistent with theoretical calculations, providing a reference for simulating and modeling other aspects of inductor design. This study offers guidance for the design optimization of integrated filter circuits and contributes to the improvement of theoretical understanding and practical implementation of inductor design in real-world applications.

References

[1] Qian Man, Wang Dong, Wang Shangheng, et al. Simulation Design and Structure Optimization of High Frequency Hollow Coil Inductor [J]. Magnetic Materials and Devices, 2022 (04).

[2] Yu Zhong, Research on key technology of magnetic integrated mount magnetic shield power inductor and application demonstration. Sichuan Province, Guang 'an Huaying Mountain Lingchuang Electronic Co., LTD., 2021-03-29.

[3] Kai Jian, Zhang Chao, Zhang Fengping, et al. Design of High Frequency High Current Hollow Inductor [J]. Magnetic Materials and Devices, 2023, (02).

[4] Hu F. Study on magnetic properties and loss mechanism of soft magnetic composites for Special magnetic components [D]. Anhui University, 2020.

[5] Fuzhou Xinxiangwei Electronic Technology Co., LTD. Through-core capacitor filter: CN202010699734.9 [P]. 2020-10-13.

[6] Shenzhen Shunluo Electronics Co., LTD. A chip inductor and its manufacturing method: CN202211486427.8 [P]. 2023-03-14.

[7] He Xiangui, Small size RF inductors. Shenzhen Shunluo Electronics Co., LTD., Guangdong Province, 2019-06-06.

[8] Chen Yang. Research on Key Technology of Power Inductor Based on Glass Medium [D]. Ningbo University, 2021.

[9] Zheng L. Preparation of NiZn ferrite film by rotating spraying method and its application in thin film inductors [D]. University of Electronic Science and Technology of China, 2020.

[10] Gao Qi, Zhou Guoyun, Wei Wei, et al. Fabrication of Solenoid core inductor for Printed Circuit Board [J]. Electronic Components and Materials, 2022, 41(12): 1346-1350.

[11] Zhou Xiaoyan, Liu Shikun, Zhang Shutian, et al. Theoretical Analysis and visualization of Magnetic Field Uniformity Distribution of Finite Length Solenoid [J]. University Physics, 2021, 40(06): 76-81.

[12] Liu Shikun, Zhang Shutian, Sun Min, et al. Magnetic field diagonally wound Solenoid [J]. Physics and Engineering, 2020, 32(06): 66-70.